

Supplementary Material for "Sources and effects of fluids
in continental retrograde shear zones: Insights from the
Kuckaus Mylonite Zone, Namibia"

C. A. Stenvall¹, A. Fagereng^{1,2}, J. F. A. Diener², C. Harris² and P. E.
Janney²

¹School of Earth & Ocean Sciences, Cardiff University, Wales, United
Kingdom

²Department of Geological Sciences, University of Cape Town, Private Bag
X3, Rondebosch 7701, South Africa

March 5, 2020

Contents of this file

1. Figure S1
2. Table S1 to S3

Additional Supporting Information (File uploaded separately)

1. Caption for Table S4

Introduction Supporting information includes additional isocon graphs (Figure S1), a table of samples with $\delta^{18}\text{O}$, aluminium saturation index, and rocktype (Table S1), a table of bulk rock major- and trace element compositions (Table S2) and a table of changes in element concentrations and mass (Table S3). An additional table to support Figure 11 is provided as a .xlsx file (Table S4).

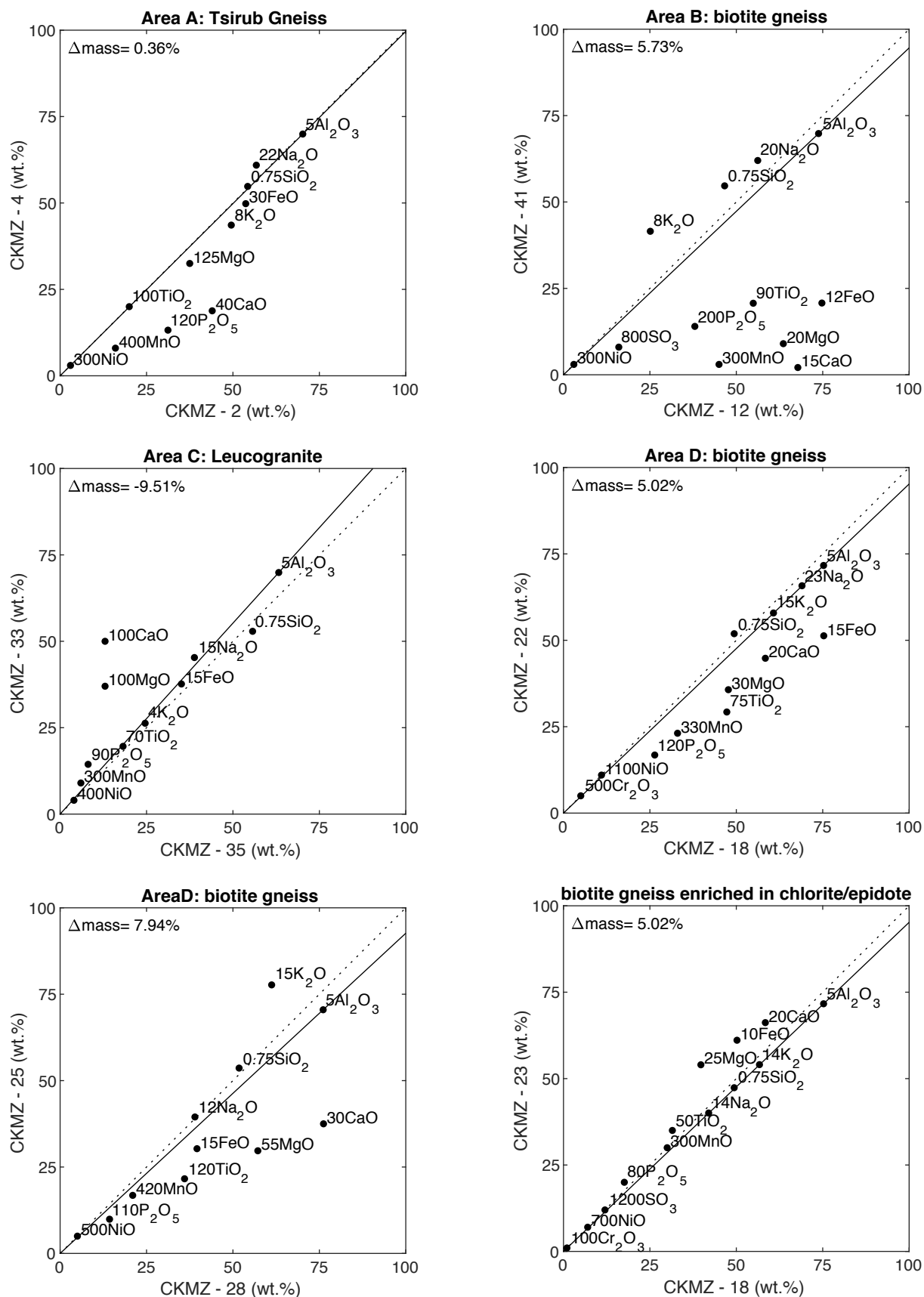


Figure S1: Additional isocon graphs.

Table S1

Whole rock oxygen isotope compositions						
CKMZ	Area	ASI	$\delta^{18}\text{O}$ (‰)	Protolith	Description	Latitude (S), Longitude (E)
2	A	1.08	9.8	Tsirub Gneiss	Migmatitic	026°48'05.8", 015°57'21.0"
3	A	1.22	9.6	Tsirub Gneiss	Protomylonite	026°48'06.6", 015°57'20.3"
4	A	1.24	8.9	Tsirub Gneiss	Ultramylonite	026°48'07.1", 015°57'20.2"
5	A	1.21	8.3	Leucogranite	Brittle deformation	026°48'06.9", 015°57'19.3"
7	A	1.14	5.4	Leucogranite	Brittle deformation	026°48'07.0", 015°57'19.1"
8	A	1.06	8.4	Leucogranite	Mylonite	026°48'06.4", 015°57'17.7"
9	A	0.93	9.0	biotite gneiss	Protomylonite (green)	026°48'06.7", 015°57'17.7"
10	A	1.10	10.0	biotite gneiss	Ultramylonite	026°48'06.7", 015°57'17.9"
11	A	1.15	8.8	biotite gneiss	Protomylonite (pink)	026°48'07.0", 015°57'18.3"
12	A	0.91	9.0	biotite gneiss	Migmatitic	026°48'06.9", 015°57'16.4"
39	B	1.17	9.3	biotite gneiss	Protomylonite	026°48'29.4", 015°57'48.1"
40	B	1.11	8.2	biotite gneiss	Mylonite	026°48'29.7", 015°57'48.9"
41	B	1.27	8.8	biotite gneiss	Ultramylonite	026°48'28.5", 015°57'48.7"
42	B	1.30	9.3	Leucogranite	Ultramylonite	026°48'28.4", 015°57'48.7"
43	B	1.11	8.5	Leucogranite	Mylonite	026°48'28.6", 015°57'49.0"
44	B	1.24	10.6	Leucogranite	Protomylonite	026°48'28.4", 015°57'49.0"
46	B	1.11	7.1	biotite gneiss	Mylonite (pink)	026°48'29.7", 015°57'50.0"
47	B	1.53	11.5	Leucogranite	Undeformed	026°48'26.3", 015°57'52.4"
31	C	1.17	13.1	Tsirub Gneiss	Protomylonite	026°48'32.4", 015°58'04.3"
32	C	1.15	11.5	Tsirub Gneiss	Mylonite	026°48'32.4", 015°58'04.3"
33	C	1.08	11.8	Leucogranite	Ultramylonite	026°48'32.4", 015°58'04.3"
34	C	1.17	12.1	Leucogranite	Mylonite	026°48'32.4", 015°58'04.3"
35	C	1.13	12.6	Leucogranite	Protomylonite	026°48'32.4", 015°58'04.3"
18	D	1.03	8.6	biotite gneiss	Migmatitic	026°49'12.4", 015°58'30.0"
19	D	1.07	7.7	biotite gneiss	Migmatitic	026°49'12.4", 015°58'30.0"
20	D	1.06	8.8	biotite gneiss	Protomylonite	026°49'12.4", 015°58'30.0"
21	D	1.09	9.2	biotite gneiss	Protomylonite	026°49'12.5", 015°58'29.9"
22	D	1.11	9.3	biotite gneiss	Protomylonite	026°49'12.5", 015°58'29.9"
23	D	1.08	9.4	biotite gneiss	Mylonite (green)	026°49'12.5", 015°58'29.9"
24	D	1.03	9.4	biotite gneiss	Ultramylonite	026°49'12.5", 015°58'29.9"
25	D	1.06	9.5	biotite gneiss	Ultramylonite	026°49'12.5", 015°58'29.9"
26	D	1.08	9.3	biotite gneiss	Ultramylonite	026°49'12.5", 015°58'29.9"
27	D	1.09	10.0	biotite gneiss	Mylonite	026°49'12.5", 015°58'29.9"
28	D	1.06	9.0	biotite gneiss	Migmatitic	026°49'12.6", 015°58'29.9"
29	D	1.08	9.9	biotite gneiss	Protomylonite	026°49'12.6", 015°58'29.9"

Quartz oxygen isotope compositions						
CKMZ	Area	$\delta^{18}\text{O}$ (‰)	Host rock	Description	Latitude (S), Longitude (E)	
6	A	-1.2	Leucogranite	Quartz vein	026°48'07.2",	015°57'19.1"
13	-	11.6	Leucogranite	Quartz vein	026°48'55.5",	015°58'33.9"
38	B	4.2	biotite gneiss	Quartz vein	026°48'29.4",	015°57'48.1"
45	B	8.4	biotite gneiss	Quartz vein	026°48'29.7",	015°57'50.0"
36	C	9.8	Tsirub Gneiss	Quartz vein	026°48'32.4",	015°58'04.3"
20	D	9.0	biotite gneiss	Quartz vein	026°49'12.4",	015°58'30.0"
30	D	10.3	biotite gneiss	Quartz vein	026°48'58.9",	015°58'32.3"
48	-	11.2	Tsirub Gneiss	Quartz vein	026°48'23.2",	015°57'57.9"
49	D	9.0	biotite gneiss	Quartz vein	026°48'23.2",	015°57'57.9"

Table S2

Area Sample (wt. %)	A	3	4	5	7	8	9	10	11	12
SiO ₂	72.35	74.38	73.06	77.25	75.01	72.85	63.64	70.98	73.57	62.16
TiO ₂	0.20	0.13	0.20	0.05	0.07	0.05	0.63	0.28	0.11	0.61
Al ₂ O ₃	14.04	13.90	13.99	12.53	12.83	15.04	14.55	13.92	13.81	14.76
Fe ₂ O ₃	1.79	1.31	1.66	0.76	0.78	0.77	5.18	2.39	0.78	6.23
MnO	0.04	0.03	0.02	0.03	0.01	0.01	0.15	0.02	0.01	0.15
MgO	0.30	0.25	0.26	0.07	0.15	-0.02	2.84	0.35	0.19	3.18
CaO	1.10	0.66	0.47	0.09	0.06	0.09	3.96	0.85	0.17	4.52
Na ₂ O	2.58	3.37	2.77	2.84	0.28	6.49	2.76	2.44	2.24	2.81
K ₂ O	6.19	4.29	5.45	5.07	9.92	3.08	3.68	6.51	7.46	3.14
P ₂ O ₅	0.26	0.11	0.11	0.05	0.02	0.02	0.23	0.10	0.03	0.19
SO ₃	-	-	-	-	-	-	0.01	-	-	0.02
Cr ₂ O ₃	-	-	-	-	-	-	0.02	-	0.02	0.01
NiO	0.01	0.01	0.01	0.01	0.01	0.01	0.02	0.01	0.03	0.01
H ₂ O ⁻	0.20	0.23	0.31	0.15	0.15	0.22	0.12	0.19	0.05	0.08
LOI	0.62	0.84	1.09	0.54	0.60	0.43	1.34	0.90	0.62	1.17
Total	99.67	99.52	99.41	99.45	99.90	99.04	99.12	98.95	99.08	99.04
(ppm)										
Zn	38		25					20		68
Cu	<5		<5					16		<5
Ni	<5		<5					<5		14
Mo	<5		<5					<5		<5
Nb	11		12					12		17
Zr	125		151					274		182
Y	17		53					10		51
Sr	125		143					244		406
Rb	225		183					181		112
U	<5		<5					<5		<5
Th	15		37					41		12
Pb	40		42					42		17
Co	<5		<5					<5		18
Mn	270		185					185		1237
Cr	18		16					15		90
V	24		19					34		120
F	393		362					314		881
S	289		358					275		367
Cl	142		107					112		168
Sc	5		6					5		20
Ba	598		597					1291		950

Table S2 (cont.)

Area Sample (wt. %)	B 39	39	40	41	42	43	44	46	47
SiO ₂	88.78	88.75	71.70	72.89	72.21	76.30	77.34	71.34	79.80
TiO ₂	0.14	0.13	0.29	0.23	0.28	0.14	0.13	0.07	0.30
Al ₂ O ₃	4.84	4.56	13.80	13.96	14.18	11.78	11.33	15.22	9.12
Fe ₂ O ₃	1.43	1.34	2.36	1.73	2.28	1.22	1.62	0.61	2.56
MnO	0.02	0.02	0.03	0.01	0.02	0.02	0.02	0.03	0.03
MgO	0.18	0.20	0.55	0.34	0.45	0.37	0.28	0.24	0.41
CaO	0.15	0.15	0.31	0.14	0.10	0.24	0.10	0.11	0.14
Na ₂ O	0.75	0.76	3.24	3.10	3.47	2.01	0.97	3.33	0.25
K ₂ O	2.35	2.21	6.05	5.19	4.61	6.32	6.79	7.44	4.90
P ₂ O ₅	0.07	0.07	0.10	0.07	0.04	0.18	0.10	0.04	0.15
SO ₃	0.02	0.00	0.00	0.01	0.01	0.00	0.00	0.00	0.00
Cr ₂ O ₃	0.02	0.00	0.00	0.00	0.00	0.00	0.00	0.00	0.00
NiO	0.06	0.01	0.01	0.01	0.01	0.01	0.01	0.01	0.01
H ₂ O ⁻	0.02	0.07	0.07	0.12	0.17	0.06	0.08	0.08	0.10
LOI	0.53	0.58	0.73	1.38	1.40	0.66	0.79	0.58	1.15
Total	99.36	98.86	99.24	99.17	99.22	99.31	99.56	99.10	98.92
(ppm)									
Zn	10	10	26	23	31				42
Cu	6	6	<5	<5	<5				<5
Ni	<5	<5	<5	<5	<5				<5
Mo	<5	<5	<5	<5	<5				<5
Nb	<5	<5	13	15	16				18
Zr	123	123	278	177	240				151
Y	8	8	35	39	37				12
Sr	46	46	126	89	87				59
Rb	73	73	175	250	237				248
U	<5	<5	8	<5	5				<5
Th	<5	<5	86	42	55				22
Pb	16	16	47	27	30				26
Co	<5	<5	<5	<5	<5				<5
Mn	160	160	246	78	114				249
Cr	39	39	13	10	13				32
V	19	19	30	27	34				23
F	395	395	369	358	361				465
S	411	411	267	459	308				276
Cl	230	230	105	100	97				93
Sc	5	5	6	5	6				<5
Ba	383	383	751	546	638				519

Table S2 (cont.)

Area Sample (wt.%)	C 31	32	33	34	35
SiO ₂	66.36	71.58	70.52	72.25	74.25
TiO ₂	0.54	0.34	0.28	0.27	0.26
Al ₂ O ₃	15.03	13.53	13.98	13.59	12.65
Fe ₂ O ₃	4.15	2.69	2.51	2.05	2.34
MnO	0.07	0.05	0.03	0.02	0.02
MgO	1.11	0.63	0.37	0.38	0.13
CaO	1.51	0.45	0.50	0.38	0.13
Na ₂ O	2.75	3.24	3.02	3.02	2.59
K ₂ O	5.13	5.22	6.57	5.51	6.15
P ₂ O ₅	0.28	0.07	0.16	0.08	0.09
SO ₃	0.00	0.01	0.00	0.00	0.00
Cr ₂ O ₃	0.02	0.00	-	-	0.00
NiO	0.02	0.01	0.01	0.01	0.01
H ₂ O ⁻	0.19	0.18	0.12	0.24	0.12
LOI	1.79	1.29	0.81	1.08	0.76
Total	98.95	99.29	98.89	98.89	99.50
(ppm)					
Zn	55		28		12
Cu	19		<5		<5
Ni	5		<5		<5
Mo	<5		<5		<5
Nb	29		12		16
Zr	191		310		134
Y	29		29		15
Sr	161		125		69
Rb	202		219		220
U	<5		<5		<5
Th	10		67		25
Pb	31		38		31
Co	<5		<5		<5
Mn	587		206		116
Cr	53		10		17
V	55		27		29
F	661		385		353
S	329		276		326
Cl	138		104		122
Sc	12		5		5
Ba	742		899		780

Table S2 (cont.)

Area Sample (wt.%)	D 18	19	20	21	22	23	24	25	26	27	28	29
SiO ₂	65.85	68.17	69.10	61.98	69.21	63.15	68.44	71.50	70.54	70.41	69.04	68.40
TiO ₂	0.63	0.39	0.29	0.89	0.39	0.70	0.40	0.18	0.18	0.34	0.30	0.28
Al ₂ O ₃	15.05	14.67	15.00	14.83	14.33	15.49	14.58	14.10	14.72	14.10	15.22	15.12
Fe ₂ O ₃	5.02	3.59	2.95	7.79	3.42	6.11	3.61	2.02	2.03	3.00	2.64	2.42
MnO	0.10	0.07	0.05	0.12	0.07	0.10	0.07	0.04	0.04	0.06	0.05	0.05
MgO	1.59	1.45	1.01	2.32	1.19	2.16	1.23	0.54	0.56	1.14	1.04	0.85
CaO	2.92	2.20	2.74	2.45	2.24	3.31	2.17	1.25	1.26	2.22	2.54	1.16
Na ₂ O	3.00	3.19	3.29	2.62	2.86	3.30	4.66	3.29	3.31	2.96	3.25	2.50
K ₂ O	4.05	4.13	3.47	4.49	3.86	2.69	2.36	5.18	5.51	3.75	4.08	7.22
P ₂ O ₅	0.22	0.14	0.13	0.13	0.14	0.25	0.18	0.09	0.09	0.13	0.13	0.15
SO ₃	0.01	0.00	0.01	0.01	0.00	0.01	0.00	0.00	0.00	0.00	0.01	-
Cr ₂ O ₃	0.01	0.01	0.00	0.02	0.01	0.01	0.03	0.00	0.00	0.01	-	0.00
NiO	0.01	0.01	0.01	0.01	0.01	0.01	0.01	0.01	0.01	0.01	0.01	0.01
H ₂ O ⁻	0.10	0.09	0.09	0.12	0.10	0.14	0.12	0.10	0.12	0.12	0.09	0.12
LOI	0.77	1.24	1.01	1.56	1.06	1.68	1.21	0.76	0.83	1.11	1.07	0.97
Total	99.34	99.35	99.15	99.34	98.90	99.11	99.06	99.04	99.20	99.36	99.46	99.24
(ppm)												
Zn	59						41				34	
Cu	37						5				<5	
Ni	14						<5				<5	
Mo	<5						<5				<5	
Nb	22						11				8	
Zr	151						149				126	
Y	54						16				7	
Sr	372						297				414	
Rb	176						115				152	
U	<5						<5				<5	
Th	17						11				8	
Pb	17						12				17	
Co	10						5				<5	
Mn	812						543				399	
Cr	48						36				27	
V	91						54				59	
F	761						452				428	
S	322						281				282	
Cl	137						112				113	
Sc	11						8				<5	
Ba	1195						684				1355	

Table S3

Area A Absolute change in concentration (%) (after Spruzeniece and Piazzolo, 2015)

Sample	Against 2		Against 47			Against 12		
	3	4	5	7	8	9	10	11
SiO ₂	3.8	1.3	-29.5	-33.2	-44.6	3.8	21.0	26.5
TiO ₂	-32.3	0.2	-88.5	-82.3	-89.2	4.9	-51.0	-80.2
Al ₂ O ₃								
Fe ₂ O ₃	-26.4	-6.7	-78.3	-78.3	-81.7	-15.7	-59.4	-86.7
MnO	-19.4	-34.5	-29.0	-71.8	-87.0	0.5	-84.4	-92.8
MgO	-16.1	-13.5	-87.7	-73.1	-102.3	-9.7	-88.3	-93.5
CaO	-39.4	-57.6	-54.0	-71.9	-59.4	-11.2	-80.0	-96.1
Na ₂ O	32.3	8.1	725.6	-20.2	1468.5	-0.3	-7.9	-15.0
K ₂ O	-30.0	-11.8	-24.7	44.0	-61.9	18.8	119.6	153.6
P ₂ O ₅	-54.8	-56.9	-74.6	-93.0	-92.4	20.4	-42.4	-82.5
SO ₃						-62.0		
Cr ₂ O ₃						60.2		79.2
NiO	-45.8	-46.3	-16.3	-28.5	-38.9	89.8	-7.1	343.5
H ₂ O ⁻	15.3	57.9	10.3	8.9	35.6	65.9	159.1	-23.3
LOI	37.9	77.4	-66.1	-62.8	-77.4	15.9	-19.0	-43.9
Zn		-32.4					-69.2	
Cu								
Ni								
Mo								
Nb		2.4					-25.1	
Zr		20.6					60.1	
Y		220.1					-80.0	
Sr		15.0					-36.4	
Rb		-18.5					72.4	
U								
Th		156.0					268.5	
Pb		5.0					156.1	
Co								
Mn		-31.4					-84.1	
Cr		-15.6					-82.4	
V		-20.6					-69.5	
F		-7.6					-62.2	
S		24.5					-20.6	
Cl		-24.3					-29.1	
Sc		23.5					-74.9	
Ba		0.2					44.0	

Total mass change (%) (after Spruzeniece and Piazzolo, 2015)

Sample	3	4	5	7	8	9	10	11
Mass change (%)	1.0	0.3	-27.2	-28.9	-39.4	1.4	6.0	6.9

Table S3 (cont.)

Area B Absolute change in concentration (%) (after Spruzeniece and Piazzolo, 2015)

Sample	Against 12			Against 47		
	40	46	41	42	43	44
SiO ₂	23.4	11.3	24.0	-41.8	-26.0	-22.0
TiO ₂	-48.1	-88.4	-59.2	-39.7	-62.7	-64.0
Al ₂ O ₃						
Fe ₂ O ₃	-59.4	-90.5	-70.6	-42.9	-63.0	-49.1
MnO	-79.2	-80.8	-92.3	-70.6	-49.0	-45.3
MgO	-81.4	-92.8	-88.6	-28.7	-30.5	-45.5
CaO	-92.6	-97.5	-96.8	-54.7	31.1	-43.2
Na ₂ O	23.3	15.0	16.5	788.8	520.7	210.6
K ₂ O	105.8	129.4	74.6	-39.5	0.0	11.7
P ₂ O ₅	-42.9	-78.5	-63.4	-82.2	-9.9	-46.4
SO ₃	-120.1	-93.8	-47.3	94.2	-180.1	-72.7
Cr ₂ O ₃	-91.1	-108.3	-82.4	-83.8	-80.0	-59.0
NiO	-6.0	-25.4	-21.0	-35.3	-19.9	-6.3
H ₂ O ⁻	1.5	6.5	62.8	11.2	-51.5	-34.8
LOI	-33.8	-52.0	24.3	-21.4	-55.7	-44.7
Zn	-58.3		-64.8	-51.6		
Cu						
Ni						
Mo						
Nb	-16.0		-4.9	-40.7		
Zr	63.7		2.7	2.1		
Y	-27.6		-20.5	97.5		
Sr	-66.9		-76.7	-4.5		
Rb	68.0		136.7	-38.7		
U						
Th	688.2		280.7	64.2		
Pb	188.2		66.3	-25.7		
Co						
Mn	-78.7		-93.3	-70.5		
Cr	-84.5		-88.5	-73.2		
V	-73.4		-76.0	-6.2		
F	-55.2		-57.1	-50.0		
S	-22.3		32.3	-28.1		
Cl	-32.9		-37.1	-33.4		
Sc	-67.9		-74.5			
Ba	-15.5		-39.2	-21.0		

Total mass change (%) (after Spruzeniece and Piazzolo, 2015)

Sample	40	46	41		42	43	44
Mass change (%)	6.9	-3.0	5.7		-35.7	-22.6	-19.5

Table S3 (cont.)

Area C Absolute change in concentration (%) (after Spruzeniec and Piazzolo, 2015)

Sample	Against 31		Against 35	
	32	33	33	34
SiO ₂	19.9	14.2	-14.1	-9.4
TiO ₂	-29.1	-42.9	-2.9	-5.3
Al ₂ O ₃				
Fe ₂ O ₃	-27.8	-34.9	-3.0	-18.3
MnO	-29.2	-56.5	61.3	5.8
MgO	-37.0	-64.5	155.0	173.3
CaO	-67.0	-64.4	249.9	174.0
Na ₂ O	30.6	17.9	5.4	8.7
K ₂ O	13.3	37.8	-3.5	-16.6
P ₂ O ₅	-72.2	-37.2	60.3	-17.2
SO ₃	285.5	-154.3	-192.1	41.0
Cr ₂ O ₃	-87.0			
NiO	-41.3	-49.3	7.5	-6.0
H ₂ O ⁺	0.9	-33.7	-8.1	86.2
LOI	-19.9	-51.0	-2.5	33.4
Zn		-45.5	115.6	
Cu				
Ni				
Mo				
Nb		-53.7	-30.9	
Zr		74.8	110.0	
Y		7.8	76.6	
Sr		-16.2	63.1	
Rb		16.1	-10.0	
U				
Th		630.6	142.7	
Pb		29.9	12.1	
Co				
Mn		-62.3	60.7	
Cr		-80.3	-48.9	
V		-48.1	-15.7	
F		-37.4	-1.4	
S		-9.9	-23.5	
Cl		-18.9	-22.9	
Sc		-53.3	4.2	
Ba		30.3	4.2	

Total mass change (%) (after Spruzeniec and Piazzolo, 2015)

Sample	32	33		33	34
Mass change (%)	11.1	7.5		-9.6	-6.9

Table S3 (cont.)

Area D

Absolute change in concentration (%) (after Spruzeniece and Piazzolo, 2015)

Sample	Against 18					Against 28				
	19	20	21	22	23	24	25	26	27	29
SiO ₂	6.2	5.3	-4.5	10.3	-6.8	3.5	11.8	10.0	10.0	-0.3
TiO ₂	-36.7	-54.4	43.0	-35.5	7.8	38.4	-35.2	22.5	22.5	-6.9
Al ₂ O ₃										
Fe ₂ O ₃	-26.6	-41.1	57.4	-28.5	18.2	42.8	-17.5	22.7	22.7	-7.7
MnO	-26.0	-45.6	18.1	-23.5	-1.4	47.6	-22.2	40.3	40.3	0.7
MgO	-6.4	-36.3	48.4	-21.0	31.9	24.2	-44.0	18.3	18.3	-17.5
CaO	-22.5	-5.7	-14.9	-19.3	10.3	-11.0	-46.9	-5.9	-5.9	-54.2
Na ₂ O	9.2	9.9	-11.4	0.2	6.9	49.8	9.3	-1.6	-1.6	-22.7
K ₂ O	4.5	-14.0	12.3	0.1	-35.5	-39.5	37.1	-0.8	-0.8	78.0
P ₂ O ₅	-36.9	-41.0	-42.8	-34.7	11.2	44.9	-27.7	6.9	6.9	20.2
SO ₃	-59.2	20.7	-9.5	-89.6	-51.7	-120.5	-36.0	-79.0	-79.0	
Cr ₂ O ₃	-10.7	-62.3	126.4	-21.9	-15.4					
NiO	-23.4	-24.6	-7.8	-30.6	-19.4	32.0	6.7	20.3	20.3	15.1
H ₂ O ⁻	-12.1	-13.1	15.4	-0.8	34.7	37.8	16.8	40.1	40.1	28.6
LOI	63.9	31.1	104.9	44.5	110.9	17.6	-23.8	11.6	11.6	-9.0
Zn						26.9				
Cu										
Ni										
Mo										
Nb						50.0				
Zr						22.8				
Y						151.4				
Sr						-25.1				
Rb						-21.1				
U										
Th						50.5				
Pb						-26.8				
Co										
Mn						41.9				
Cr						39.7				
V						-3.7				
F						10.2				
S						4.0				
Cl						3.8				
Sc										
Ba						-47.4				

Total mass change (%) (after Spruzeniece and Piazzolo, 2015)

Sample	19	20	21	22	23	24	25	26	27	29
Mass change (%)	2.6	0.3	1.4	5.0	-2.9	4.4	7.9	3.4	7.9	0.6

Table S4 This table is available as a .xlsx file and contains para- and orthogneiss whole-rock $\delta^{18}\text{O}$ values used for Figure 11 (Beckinsale, Evans, Thorpe, Gibbons, & Harmon, 1984; Cartwright & Barnicoat, 2003; Cartwright & Buick, 1999; Cartwright, Valley, & Hazelwood, 1993; Curtis, Harris, Trumbull, De Beer, & Mudzanani, 2013; Eiler & Valley, 1994; Fagereng, Harris, La Grange, & Stevens, 2008; Khan et al., 2019; Lackey, Valley, & Saleeby, 2005; Longstaffe & Schwarcz, 1977; McCaig, Wickham, & Taylor, 1990; Prame & Pohl, 1994; Prochaska, Bechtel, & Klötzli, 1992; Read & Cartwright, 2000; Rehman et al., 2014; Stenvall, Fagereng, & Diener, 2019).

References

- Beckinsale, R., Evans, J., Thorpe, R., Gibbons, W., & Harmon, R. (1984). Rb-Sr whole-rock isochron ages, $\delta^{18}\text{O}$ values and geochemical data for the Sarn Igneous Complex and the Parwyd gneisses of the Mona Complex of Llŷn, N Wales. *Journal of the Geological Society*, *141*(4), 701–709.
- Cartwright, I., & Barnicoat, A. C. (2003). Geochemical and stable isotope resetting in shear zones from Täschalp: constraints on fluid flow during exhumation in the Western Alps. *Journal of Metamorphic Geology*, *21*(2), 143–161.
- Cartwright, I., & Buick, I. S. (1999). The flow of surface-derived fluids through Alice Springs age middle-crustal ductile shear zones, Reynolds Range, central Australia. *Journal of Metamorphic Geology*, *17*(4), 397–414.
- Cartwright, I., Valley, J. W., & Hazelwood, A.-M. (1993). Resetting of oxybarometers and oxygen isotope ratios in granulite facies orthogneisses during cooling and shearing, Adirondack Mountains, New York. *Contributions to Mineralogy and Petrology*, *113*(2), 208–225.
- Curtis, C. G., Harris, C., Trumbull, R. B., De Beer, C., & Mudzanani, L. (2013). Oxygen isotope diversity in the anorogenic Koegel Fontein complex of South Africa: a case for basement control and selective melting for the production of low- $\delta^{18}\text{O}$ magmas. *Journal of Petrology*, *54*(7), 1259–1283.
- Eiler, J. M., & Valley, J. W. (1994). Preservation of premetamorphic oxygen isotope ratios in granitic orthogneiss from the Adirondack Mountains, New York, USA. *Geochimica*

- et Cosmochimica Acta*, 58(24), 5525–5535.
- Fagereng, Å., Harris, C., La Grange, M., & Stevens, G. (2008). Stable isotope study of the Archaean rocks of the Vredefort impact structure, central Kaapvaal Craton, South Africa. *Contributions to Mineralogy and Petrology*, 155(1), 63–78.
- Khan, T., Ahmad, A., Rehman, H. U., Chaudhry, M. N., Murata, M., & Zafar, M. (2019). Rb-Sr and Oxygen Isotope Study of the Swat Granite Gneisses (Pakistan): Implications for the Magmatic Source and Tectonic Setup. In *Petrogenesis and exploration of the earth's interior* (pp. 41–43). Springer.
- Lackey, J. S., Valley, J. W., & Saleeby, J. B. (2005). Supracrustal input to magmas in the deep crust of Sierra Nevada batholith: Evidence from high- $\delta^{18}\text{O}$ zircon. *Earth and Planetary Science Letters*, 235(1-2), 315–330.
- Longstaffe, F. J., & Schwarcz, H. P. (1977). $^{18}\text{O}/^{16}\text{O}$ of Archean clastic metasedimentary rocks: a petrogenetic indicator for Archean gneisses? *Geochimica et Cosmochimica Acta*, 41(9), 1303–1312.
- McCaig, A. M., Wickham, S. M., & Taylor, H. P. (1990). Deep fluid circulation in alpine shear zones, Pyrenees, France: field and oxygen isotope studies. *Contributions to Mineralogy and Petrology*, 106(1), 41–60.
- Prame, W., & Pohl, J. (1994). Geochemistry of pelitic and psammopelitic Precambrian metasediments from southwestern Sri Lanka: implications for two contrasting source-terrains and tectonic settings. *Precambrian Research*, 66(1-4), 223–244.
- Prochaska, W., Bechtel, A., & Klötzli, U. (1992). Phyllonite formation and alteration of gneisses in shear zones (Gleinalmkristallin, Eastern Alps/Austria). *Mineralogy and Petrology*, 45(3-4), 195–216.
- Read, C., & Cartwright, I. (2000). Meteoric fluid infiltration in the middle crust during shearing: examples from the Arunta Inlier, central Australia. *Journal of Geochemical Exploration*, 69, 333–337.
- Rehman, H. U., Tanaka, R., O'Brien, P. J., Kobayashi, K., Tsujimori, T., Nakamura, E., . . . Kaneko, Y. (2014). Oxygen isotopes in Indian Plate eclogites (Kaghan Valley, Pakistan): Negative $\delta^{18}\text{O}$ values from a high latitude protolith reset by Himalayan metamorphism. *Lithos*, 208, 471–483.
- Spruzeniece, L., & Piazzolo, S. (2015). Strain localization in brittle-ductile shear zones: fluid-abundant vs. fluid-limited conditions (an example from Wyangala area,

Australia). *Solid Earth*, 6(3), 881.

Stenvall, C. A., Fagereng, Å., & Diener, J. F. (2019). Weaker than weakest: on the strength of shear zones. *Geophysical Research Letters*, 46(13), 7404–7413.